HHS Public Access

Author manuscript

Cancer Immunol Res. Author manuscript; available in PMC 2023 July 03.

Published in final edited form as:

Cancer Immunol Res. 2023 January 03; 11(1): 109–122. doi:10.1158/2326-6066.CIR-22-0391.

Increased CaMKK2 expression is an adaptive response that maintains the fitness of tumor-infiltrating natural killer cells

Patrick K. Juras[1], **Luigi Racioppi**[2,3], **Debarati Mukherjee**[1], **Sandeep Artham**[1], **Xia Gao**[1,4], **Laura Akullian D'Agostino**[5], **Ching-Yi Chang**[1], **Donald P. McDonnell**[1]

[1]Department of Pharmacology and Cancer Biology, Duke University School of Medicine, Durham, NC 27710, USA

[2]Department of Medicine, Division of Hematological Malignancies and Cellular Therapy, Duke University School of Medicine, Durham, NC, 27710, USA

[3]Department of Molecular Medicine and Medical Biotechnology, University of Naples Federico II, Naples, 80131, Italy

[4]Children's Nutrition Research Center, Department of Pediatrics, Baylor College of Medicine, Houston, TX 77030, USA

[5]Small Molecule Drug Discovery, Bristol Myers Squibb, 200 Cambridge Park Drive, Cambridge, MA 02140, USA

Abstract

Calcium/calmodulin-dependent protein kinase kinase 2 (CaMKK2) is a key regulator of energy homeostasis in several cell types. Expression of this enzyme in tumor cells promotes proliferation and migration, and expression in tumor-associated immune cells facilitates M2 macrophage polarization and the development of myeloid-derived suppressor cells. Thus, there has been interest in developing CaMKK2 inhibitors as potential anticancer therapeutics. One impediment to clinical development of these agents is that the roles of CaMKK2 in other cellular compartments within the tumor immune microenvironment remain to be established. We report herein that CaMKK2 is expressed at low basal levels in natural killer (NK) cells but is upregulated in tumor-infiltrating NK cells where it suppresses apoptosis and promotes proliferation. NK cell–intrinsic deletion of CaMKK2 increased metastatic progression in several murine models, establishing a critical role for this enzyme in NK cell–mediated antitumor immunity. Ablation of the CaMKK2 protein, but not inhibition of its kinase activity, resulted in decreased NK-cell survival. These results indicate an important scaffolding function for CaMKK2 in NK cells and suggest that competitive CaMKK2 inhibitors and ligand-directed degraders (LDDs) are likely to have distinct therapeutic utilities. Finally, we determined that intracellular lactic acid is a key driver of CaMKK2 expression, suggesting that upregulated expression of this enzyme is an adaptive mechanism by which tumor-infiltrating NK cells mitigate the deleterious effects of a lactic acid–rich tumor microenvironment. The findings of this study should inform strategies to manipulate the CaMKK2 signaling axis as a therapeutic approach in cancer.

Corresponding author: Donald P. McDonnell; B238 LSRC, Durham, NC 27710; 919-684-6035; donald.mcdonnell@duke.edu.

Keywords

Natural killer cells; tumor immunology; CaMKK2; lactic acid; ligand-directed degraders (LDD)

INTRODUCTION:

Solid tumors create unique metabolic challenges that tumor-associated cells must navigate to survive and proliferate [1, 2]. Calcium/calmodulin-dependent protein kinase kinase 2 (CaMKK2) is a calcium-activated serine/threonine kinase that regulates metabolic functions through several pathways, including the AMP-activated protein kinase (AMPK) and Calcium/calmodulin-dependent protein kinase type IV (CaMKIV) pathways [3, 4]. Originally studied in the context of central nervous system physiology [5, 6], CaMKK2 was subsequently found to play important regulatory roles in many tissues, most notably control of gluconeogenesis in the liver [7], insulin signaling in the pancreas [8], and osteoblast activity in the bone [9]. Dysregulated CaMKK2 signaling also contributes to the pathology of several diseases, including non-alcoholic fatty liver disease (NAFLD) and tumor progression in many different cancers [3, 4]. Indeed, ectopic expression of CaMKK2 results in the suppression of anoikis [10], enhanced migratory capacity [11], and increased proliferation of cancer cells [12].

In the immune system, CaMKK2 is highly expressed in early hematopoietic stem and progenitor cells, where it promotes quiescence and suppresses differentiation [13, 14]. CaMKK2 expression in granulocyte–monocyte progenitor cells promotes monocyte lineage commitment, and its expression is attenuated as granulocytes mature [13, 15]. However, CaMKK2 remains highly expressed in monocytes and monocyte-derived macrophages, and deletion of this kinase attenuates macrophage-mediated inflammatory responses [16]. We have shown that pharmacologic inhibition of CaMKK2 prevents the accumulation of M2-like tumor-associated macrophages (TAMs) [17] while decreasing the number of myeloid-derived suppressor cells (MDSC) in the tumor microenvironment [18]. Thus, CaMKK2 contributes to tumor biology through its ability to regulate cancer cell–intrinsic biology and through its actions in specific myeloid populations [10–12, 17–19]. However, the role of CaMKK2 in other tumor-infiltrating immune populations has yet to be studied, limiting our ability to develop a complete model of how CaMKK2 influences tumor pathobiology.

Given its role in promoting tumor progression, there is interest in developing CaMKK2 inhibitors as anticancer therapeutics. The most widely used CaMKK2 antagonist, the competitive inhibitor STO-609, has shown efficacy in mouse models of breast cancer and NAFLD [17, 20]. However, the poor pharmaceutical properties of this drug coupled with its established off-target activities are an impediment to its clinical development [21]. Several new inhibitors are emerging with improved properties, and these new drugs are divided into two functional categories: ATP-competitive inhibitors of kinase function, and ligand-directed degraders (LDDs) of the enzyme. LDDs are a new class of bi-specific molecules that feature a target-binding ligand paired with a ubiquitin ligase–recruitment domain that promotes proteasomal degradation of the target protein. LDDs may offer advantages over kinase inhibitors, including activity against inhibitor-resistant cancers and enhanced target

selectivity [22, 23], although it remains to be determined whether CaMKK2-specific LDDs and competitive inhibitors are functionally equivalent. As these compounds are currently under investigation as anticancer therapeutics, it has become important to understand the effects of CaMKK2 modulation on immune cell function.

METHODS AND MATERIALS:

Mouse strains and cell lines:

The [Tg(CaMKK2-eGFP)BL/6] reporter mouse line originates from the Mutant Mouse Regional Resource Center [25] and was obtained from the lab of Luigi Racioppi (Duke University). This strain features the sequence of enhanced green fluorescent protein (eGFP), followed by a polyadenylation sequence, inserted into the mouse genomic bacterial artificial chromosome RP23-31J24 at the initiation codon of the CaMKK2 gene.

The CaMKK2$^{-/-}$ (KO) mouse strain and the CaMKK2$^{fl/fl}$ mouse strain were originally generated in the lab of Anthony Means (Baylor College of Medicine) [6] and maintained in the lab of Luigi Racioppi (Duke University). To generate NKp46-cre CaMKK2$^{fl/fl}$ mice, CaMKK2$^{fl/fl}$ mice were bred with NKp46-iCre mice originally created by Eric Vivier (Centre d'Immunologie de Marseille-Luminy) [26] and obtained (with permission) from the lab of Joseph Sun (Memorial Sloan Kettering). To generate tamoxifen-inducible CaMKK2 KO mice, CaMKK2$^{fl/fl}$ mice were bred with UBC-Cre-ERT2 mice acquired from Jackson Labs (strain #007001). ERT2$^{+/-}$ CaMKK2$^{fl/fl}$ mice were dosed with 2 mg tamoxifen citrate (Sigma-Aldrich, cat no. T9262) in corn oil via oral gavage daily for one week, and splenic CaMKK2-deficient natural killer (NK) cells were harvested 5 days after dosing ended.

NSG mice were purchased as needed from Jackson Labs (strain # 005557). WT C57BL/6 (WT) mice were purchased from Jackson Labs (strain # 000664) and propagated in-house.

The EO771 (parent) breast cancer line was acquired from the lab of Mark Dewhirst (Duke University) and last underwent IMPACT III PCR testing in 2015. EO771 cells were passaged approximately 6–8 times before experimental use. The A7C11 breast cancer cell line was acquired from the lab of Jose Conejo-Garcia (Moffitt Cancer Center) and last underwent IMPACT III PCR testing in 2019. A7C11 cells were passaged approximately 10 times before experimental use. The EO771 and A7C11 lines were cultured in RMPI 1640 (Gibco, cat no. 11-875-093) containing 10% fetal bovine serum (FBS) (Sigma cat no. F2442-500ML), 1 mM sodium pyruvate (NaPy) (Gibco, cat no. 11360070) and 0.1 mM non-essential amino acids (NEAA) (Gibco, cat no. 11140050). The B16-F10 melanoma cell line (originally from ATCC, CRL6475) was acquired from the Duke Cell Culture Facility (DCCF) and last underwent IMPACT III PCR testing in 2017. B16-F10 cells were passaged approximately 10–12 times before experimental use and were cultured in DMEM (Gibco, cat no. 11965092) containing 10% FBS, 1 mM NaPy, and 0.1 mM NEAA. The YAC-1 cell line (originally from ATCC, TIB-160) was acquired from DCCF and did not undergo validation testing. YAC-1 cells were passaged approximately 3–4 times before experimental use and were cultured in RPMI 1640 containing 10% FBS, 1 mM NaPy, 10 mM HEPES (Gibco, cat no. 15630080), and 3.6 g/L glucose (Gibco, cat no. A249001). The HEK293T cell line was acquired from ATCC and did not undergo validation testing. HEK293T cells

were passaged 10–12 times before experimental use and were cultured in DMEM containing 10% FBS, 1 mM NaPy, 0.1 mM NEAA, and 2 mM L-glutamine (Gibco, cat no. 25030081). All cells were incubated in a humidified chamber at 37°C in a 5% CO_2 atmosphere.

Creation of plasmid vector to knock-out β2m in EO771:

The EO771 cell line was engineered using CRISPR to knock-out both alleles of the β2m locus, eliminating expression of the major histocompatibility complex class I. The Lenti-Cas9-gRNA-GFP plasmid vector (Addgene plasmid #124770) was first modified to contain two specific guide RNA (gRNA) sequences targeting the mouse β2m locus. In brief, this plasmid was linearized via digestion with the BsmBI restriction enzyme, separated on a 1% agarose gel, and recovered using the QIAquick gel extraction kit (Qiagen, cat no. 28706X4). The following forward and reverse primer sets were annealed together through gradual cooling from 95 degrees:

β2M-1F: 5'-CACCGAGTATACTCACGCCACCCAC-3'

β2M-1R: 5'-AAACGTGGGTGGCGTGAGTATACTC-3'

β2M-2F: 5'-CACCGAGTCGTCAGCATGGCTCGCT-3'

β2M-2R: 5'-AAACAGCGAGCCATGCTGACGACTC-3'.

1 μL of the annealed primers was then incubated with 25 ng of the linearized plasmid in a 10 uL reaction volume at room temperature for 30 minutes in the presence of the T4 ligase. 5 μL of each ligated plasmid was incubated with 50 uL of Stbl3 homologous recombination-deficient bacteria (ThermoFisher, cat no. C737303) on ice for 30 minutes. The bacteria were then heat shocked at 42 degrees for 40 seconds, added to 300 uL of SOC media (ThermoFisher, cat no. J60255.AE), shaken at 37 degrees for 1 hour, and plated onto LB-Amp plates (100 μg/mL ampicillin). The two plates were incubated for 24 hours at 37 degrees, and 5 colonies from each plate were picked for a 24-hour expansion in 3 mL liquid LB-Amp media. The QIAprep mini prep kit (Qiagen, cat no. 27106X4) was used to isolated plasmid DNA from the 10 expanded bacteria colonies, and the samples were submitted to Eton Bio for sequencing with the "hU6" universal primer set. Using the procedure described in the next section, EO771 cells were transfected with the β2m-cas9-gRNA constructs.

Cell line modification with luciferase or β2m KO construct:

HEK293T cells were grown to 40% confluency in a 10-cm plate. To each 10 cm plate, lentivirus transduction mixture was prepared by adding the following reagents, in order, to 263 μL Opti-Mem (Gibco, cat no. 51985091): 17 μL FuGENE-6 (Promega, cat no. E2692), 280 ng VSVG envelope vector (Addgene, plasmid #8454), 2.8 μg PsPAX2 lentivirus packaging vector (Addgene, plasmid #12260), and 2.8 μg Lenti-luciferase P2A-Neo construct (Addgene, plasmid #105621) or 2.8 μg of the β2m-cas9-gRNA construct described above. The lentivirus transduction mixture was incubated for 30 minutes at RT and then added dropwise to the HEK293T plate. The luciferase construct contained a neomycin selection marker, and the β2m-cas9-gRNA construct contained an eGFP selection marker. 24 hours later, the media was aspirated and replaced with fresh DMEM media containing

30% FBS. 24 hours later, the lentivirus-containing media was recovered, passed through a 0.45 μm filter (VWR 28145-479), diluted 1:1 in DMEM, and added to B16-F10 or EO771 cell cultures. 24 hours later, the virus-containing media was aspirated, and a second round of diluted virus-containing media was added. 24 hours later, the virus-containing media was replaced with normal growth media, and transduced cells were selected using 1 week of treatment with 200–1000 μg/mL neomycin (Geneticin brand, Gibco, cat no. 10-131-027). EO771 cells with homozygous ablation of β2m were isolated using fluorescent activated cell sorting (FACS) to select for $GFP^{+}MHC\ I^{-}$.

Isolation and culture of primary mouse NK cells:

Spleens from WT or CaMKK2 KO C57BL/6 female mice aged 10–12 weeks were harvested and crushed through a 40 μm cell strainer into PBS+ 2% FBS. The EasySep Mouse NK Cell Isolation Kit (StemCell Technologies, cat no. 19855) was used to isolate NK cells through negative selection. NK-cell purity was measured using an Accuri C6 flow cytometer (BD Biosciences) to determine the percentage of purified cells expressing CD49b. The following antibodies were used: CD49b-PE (BioLegend, cat no. 103506) and isotype control (Invitrogen, cat no. 12-4888-81). NK cells were cultured in either a 50/50 mixture of EO771 TCM and normal growth media, normal growth media alone, or normal growth media containing 10 mM lactic acid (Sigma-Aldrich, cat no. L6661-100mL). Normal growth media consists of RMPI 1640 containing 10% FBS, 1 mM NaPy, 0.1 mM non-essential amino acids, 10 mM HEPES, 2 mM L-glutamine, 55 μM 2-mercaptoethanol (Gibco, cat no. 21985023), and 100 units/mL Penicillin + 100 μg/mL Streptomycin (Gibco, cat no. 15140122). Experiments requiring pH stabilization used 25 mM HEPES and 25 mM PIPES (ThermoFisher Scientific, cat no. J62195-AP) in place of 10 mM HEPES. 100 ng/mL IL2 (PeproTech, cat no. 212-12) and/or 100 ng/mL IL15 (PeproTech, cat no. 210-15) were added to the culture media depending on the experiment. All cells were incubated in a humidified chamber at 37°C in a 5% CO_2 atmosphere.

CaMKK2 inhibitors or LDDs were added to the NK-cell cultures immediately after plating. Kinase inhibitors include CC8977 (Supplementary Fig. S1A), GSKi [17], STO-609 (Thermo Scientific, cat no. J67344.LB0), and YL-36 (acquired from David Drewry at UNC). LDDs include CC3240 and CC3756 (Supplementary Fig. S1B). MCT inhibitors AZ3965 (Sigma-Aldrich, cat no. 1448671-31-5) and αCHC (Sigma-Aldrich, cat no. C2020-10G) were also added to NK-cell cultures immediately after plating. CaMKK2 inhibitors and LDDs were added at a concentration of 2.5 μM unless overwise stated. AZD3965 was added at a concentration of 500 nM, and α-cyano-4-hydroxycinnamic acid (αCHC) was added at a concentration of 5 mM.

Generation of tumor-conditioned media (TCM):

One million EO771 or A7C11 tumor cells were plated on a 10-cm cell culture dish in normal NK-cell growth media—RPMI 1640 supplemented with 10% FBS, 1 mM sodium pyruvate, 0.1 mM NEAA, 10 mM HEPES, 2 mM L-glutamine, 55 μM 2-mercaptoethanol, 100 units/mL Penicillin + 100 μg/mL Streptomycin, 100 ng/mL murine IL2, and 100 ng/mL murine IL15 and incubated at 37°C. At exactly 72 hours, the growth media was recovered from each plate, centrifuged at 2000 x g for 5 minutes, and the supernatant frozen at −80°C.

Heat-inactivated TCM was generated by incubating a 10 mL conical of TCM in a 56°C water bath for 30 minutes.

Propagation of bone marrow–derived macrophages (BMDMs):

Tibias and femurs were harvested from WT and CaMKK2 KO C57BL/6 mice and manually crushed into room temperature PBS containing 2% FBS and 2 mM EDTA. The supernatant was filtered through a 40 μm cell strainer and centrifuged at 900 x g for 5 minutes. The pellet was resuspended in ACK lysis buffer (ThermoFisher A1049201 or VWR, cat no. 10128-802) for 3 minutes to eliminate erythrocytes, diluted in 10 volumes of PBS, and centrifuged again. 18 million cells in 10 mL of media were plated on each 10 cm plate and incubated at 37°C for 6 days. BMDM media consists of DMEM supplemented with 10% FBS, 2 mM L-glutamine, 100 units/mL Penicillin + 100 μg/mL Streptomycin, and 50 ng/mL M-CSF (Peprotech, cat no. 315-02). Cells were harvested by mechanical scraping into ice cold PBS. The cells were centrifugation at 10,000 x g for 3 minutes, and the pellet was immediately frozen at −80°C for later immunoblot analysis.

Western immunoblotting:

Cell pellets from the source indicated in the corresponding figure legend were suspended in RIPA buffer (Supplementary Table S1), flash-frozen in liquid nitrogen, and rotated at 4°C for 30 minutes. 40 μg of protein per sample was resolved on a 7.5% acrylamide gel using SDS-PAGE and transferred onto a nitrocellulose membrane (LI-COR, cat no. 926-31092). The nitrocellulose membrane was blocked with 1g/L casein hydrolysate (MP Bio, cat no. 02101290) and 4.5 g/L fish gelatin (Sigma-Aldrich, cat no. G7041-100G) and then incubated with the primary antibodies listed in Supplementary Table S2. Images were captured using the LI-COR Odyssey Classic scanner and processed using LI-COR Image Studio software, version 4.0.

Tail-vein metastasis studies:

For studies that employed adoptive transfer of NK cells into NSG hosts, splenic NK cells were isolated from 10–12 week old WT, CaMKK2 KO, tamoxifen-treated ERT2^{+}, or tamoxifen-treated ERT2^{-} female mice and cultured for 24 hours in normal NK-cell growth media containing 100 ng/mL murine IL15 but not IL2. 6–7 week old female NSG mice were then injected with 250,000 live NK cells via the lateral tail vein in 100 μL HBSS without calcium or magnesium (Fisher Scientific, cat no. 14-170-112). 200 units of murine IL2 in 100 μL PBS was injected into the peritoneal cavity immediately after adoptive transfer of the NK cells and every third day thereafter to maintain NK-cell viability. This adoptive transfer protocol is a modified version of previously published methods [27, 28]. When using the B16-F10 model, 500,000 tumor cells were mixed with NK cells immediately before being injected concurrently. When using the β2m$^{-/-}$ EO771 model, 300,000 tumor cells were injected into the lateral tail vein 48 hours prior to the NK cells. For studies involving immune competent host mice with intrinsic NK cell–specific ablation of CaMKK2, no adoptive transfer of NK cells was performed and no IL2 i.p. injections were required. The only injection in these studies was 500,000 B16-F10 tumor cells into the lateral tail veins of 12 week old iCre+/− CaMKK2 wt/wt and iCre+/− CaMKK2 fl/fl females.

Following tail vein injections of tumor cells, mice were regularly anesthetized with isoflurane and intravenously administered 100 μL luciferin (Regis Technologies, cat no. 1-360243-200) at the standard concentration of 50 mM. Bioluminescence was measured using an IVIS Lumina XR optical imaging system with an exposure time of 2–3 minutes. Lungs were extracted post-mortem and processed for immune profiling in the manner described below.

Primary tumor studies:

11–12 week old CaMKK2-eGFP reporter mice were injected subcutaneously with 200,000 EO771 tumor cells in 100 μL HBSS. Upon reaching a volume of 1 cm^3, tumors and spleens were recovered and prepared for flow cytometry in the manner described above.

Harvesting and processing mouse tissues:

Various organs and tumors were extracted from mice post-mortem and homogenized for flow cytometry immune profiling of the tissue. Unless otherwise indicated, mice were 12 weeks old at the time of harvest. Prior to extraction, lungs were perfused with PBS to remove intravascular blood. All solid organs, including liver, lung, lymph nodes, and spleen were mechanically pulverized in 5 mL DMEM+5% FBS, and enzymatically digested with 1 mg/mL Collagenase A (Roche, cat no. 10103586001) and 200 units/mL DNAse I (Sigma, D5025-150KU) for 30 minutes in a 37°C shaker. The resulting cell suspensions were filtered through a 40 μm cell strainer and centrifuged at 900 x g for 5 minutes. The pellet was resuspended in ACK lysis buffer for 3 minutes to eliminate erythrocytes, resuspended in PBS, and stained for flow cytometry as described below. Blood was recovered through post-mortem cardiac puncture and stored in EDTA tubes (BD, cat no. 365974) until erythrocytes were lysed with three volumes of ACK lysing buffer for 3 minutes. The remaining blood cells were resuspended in PBS and then stained for flow cytometry. Bone marrow cells were recovered through the process described in “Propagation of BMDMs”, but cells were resuspended in PBS for flow cytometry analysis rather than plated in BMDM growth media with M-CSF.

Flow cytometry immune profiling:

The following reagents were used to prepare cells for flow cytometry. 1 million cells per well were aliquoted to a round-bottom 96 well plate and centrifuged at 900 x g for 5 minutes. Cells were resuspended in PBS containing 1:100 anti-CD16/32 (Invitrogen, cat no. 14-0161-85) and 1:100 anti-CD16.2 (BioLegend, cat no. 149502) for Fc receptor blocking, and 1:200 LIVE/DEAD Fixable Violet Dead Cell Stain (Invitrogen, cat no. L34964) as a viability marker. Cells were incubated for 15 minutes on ice, centrifuged, and resuspended in BD Horizon Brilliant Staining buffer (BD 566349) containing a combination of cell-surface fluorophore-antibody conjugates (Supplementary Table S3). Cells were incubated for 30 minutes on ice, washed with 3 volumes of PBS, centrifuged, and then permeabilized using eBioscience Fixation/Perm solution (Invitrogen, cat no. 00-5123-43 and 00-5223-56) for 30 minutes. Cells were then centrifuged and stained with a combination of intracellular fluorophore-antibody conjugates in Permeabilization Buffer (Invitrogen, cat no. 00-8333-56). Cells were finally fixed in BD Cytofix fixation buffer diluted 1:4 (BD Bioscience, cat no. 554655). Flow cytometry data was collected using the LSRFortessa X-20

flow cytometer (BD Biosciences) with BD FACSDiva software (BD Biosciences). Data was subsequently analyzed using FlowJo software version 10.7.1. The Accuri C6 flow cytometer and accompanying software (BD Biosciences) was used to collect and analyze data for the *in vitro* migration and cytotoxic assays..

CFSE proliferation assay:

NK cells were treated with 5 μM CellTrace CFSE (Invitrogen, cat no. C34554A) in RMPI media + 5% FBS for 5 minutes, washed twice with the same media, and cultured for 72 hours. NK-cells were identified by flow cytometry as live $CD45^+CD3^-NK1.1^+CD49b^+$ cells.

In vitro cytotoxicity assay:

25,000 CFSE-stained YAC-1 cells were mixed with live NK cells at a ratio of 1:25, 1:5, 1:1, and 5:1 (NK:YAC-1) in NK-cell media in a 96-well plate. The cells were co-incubated at 37°C for 4 hours and then stained with LIVE/DEAD Fixable Violet Dead Cell Stain and anti-CD45-BV605 (Invitrogen, cat no. 103139) for flow cytometry analysis. YAC-1 cells were identified as $CFSE^+$, and their viability was recorded [24].

In vitro migration assay:

500,000 live NK cells were suspended in 100 μL of normal NK-cell growth media and added to the upper insert of a transwell migration chamber with 5 μm pores (Corning, cat no. 3421). 600 μL of normal NK-cell growth media containing 0 or 250 ng/mL CCL4 (BioLegend, cat no. 554602) was added to the lower chamber, and the migration plate was incubated at 37°C for 3 hours. The total number of $CD49b^+$ cells present in the lower chamber was measured via flow cytometry.

Analysis of TCM metabolite content:

To extract metabolites, 20 μL of TCM was added to 80 μL of ice-cold water followed by 400 μL of ice-cold methanol. Samples were vortexed aggressively for 1 min and then centrifuged at 20,000 x g for 10 min at 4°C. The supernatants were transferred to new tubes and dried in a vacuum concentrator. The dry pellets were reconstituted in 30 μL of sample solvent (water:methanol:acetonitrile, 2:1:1, v/v/v) and then centrifuged at 20,000 x g 3 min at 4°C. 3 μL of supernatant was run on Liquid Chromatography using a HILIC with an Xbridge amide column (100 x 2.1 mm internal diameter, 3.5 mm; Waters) and Vanquish™ UHPL coupled to Q-Exactive-plus Mass spectrometer system (Thermo Scientific) for metabolite separation and detection. The relevant settings include heater temperature 120°C, sheath gas 30, sweep gas 3, auxiliary gas 10, and spray voltage 3.0 kV for positive mode and 2.5 kV for negative mode. Liquid chromatography–mass spectrometry peak extraction and integration were analyzed with the Compound Discoverer 3.2 software (Thermo Scientific). The integrated peak intensity was used for further data analysis.

Analysis of data from the Immunological Genome Project (ImmGen) database:

Levels of *Hcar1* mRNA (encodes GPR81) and *Slc16a1* mRNA (encodes MCT1) were compared across various splenic immune populations using bulk mRNA sequencing data

from the ImmGen database. The Gene skyline RNAseq databrowser, available on the ImmGen website, was used to visually compare mRNA levels. Populations of interest were chosen using the “Select the populations by cell types” tab. mRNA data for NK-cell subsets was generated by Tsukasa Nabekura (NK.27+/−11b+/−.Sp); mRNA data for dendritic cells was generated by Barbara Maier and Stefan Jordan (DC8+.Sp); mRNA data for monocytes was generated by Kiwook Kim (Mo.6C+II-.Bl); and mRNA data for B cells and macrophages was generated by Andrew Rhoads (B.Sp and MF.PC, respectively).

Statistical analysis:

Standard error of the mean is shown based on 2–3 biological replicates per experiment. Excel was used for statistical analysis. P-value was determined using an unpaired Student’s t-test with a significance threshold of $P<0.05$ (*$P<0.05$, **$P<0.01$, ***$P<0.005$).

Data availability statement:

All data generated in this study is available within the article and its supplementary data files or upon request from the corresponding author.

Ethics statement:

All animal work was approved by the Duke Institutional Animal Care and Use Committee and was conducted in a manner that minimizes pain and distress in the animal subjects.

RESULTS:

CaMKK2 is upregulated in tumor-infiltrating mouse NK cells

As a first step in this study, we screened for CaMKK2 expression across several immune cell types under normal physiological conditions in mice. For these initial experiments we used the [Tg(CaMKK2-eGFP)BL/6] transgenic reporter mouse line, which expresses eGFP under the control of the CaMKK2 promoter [25]. Several tissues were harvested from the CaMKK2 reporter mice and subjected to flow cytometry analysis, using a previously described gating strategy to identify ten distinct immune populations (Fig. 1A–B, Supplementary Fig. S2A–B) [17, 29]. The results from this experiment confirmed that the eGFP reporter was highly active in myeloid cells, especially macrophages (Fig. 1A, Supplementary Fig. S2A) [16, 18]. In contrast, eGFP expression was not observed in B cells or any T-cell subset. eGFP expression was also detected in a subset of mature NK cells, which expressed the typical myeloid marker CD11b (Fig. 1A, Supplementary S2A) [30]. To confirm this finding, we analyzed NK cells from spleen, blood, and bone marrow using a more stringent flow cytometry gating strategy (Supplementary Fig. S2C). The $eGFP^{high}$ subpopulation of $CD11b^{+}$ NK cells was identified in all tissues analyzed (Fig. 1B, Supplementary Fig. S2A).

We repeated the evaluation of CaMKK2 expression in tumor-infiltrating immune cells recovered from subcutaneous EO771 mammary tumors propagated in the CaMKK2 reporter mouse model. We found that NK cells recovered from these tumors showed higher eGFP expression than those recovered from the spleens of the same mice (Fig. 1C), with the levels of eGFP expression approaching the macrophage positive control (Fig. 1D). eGFP

expression in the splenic NK cells from tumor-bearing mice was similar to that found in healthy mice (Fig. 1E), strongly suggesting that upregulation of CaMKK2 promoter activity was specific to the tumor environment rather than a systemic response in tumor-bearing animals. Among tumor-infiltrating NK cells, expression of eGFP was correlated with, though not specific to, the later maturation states (Fig. 1F). However, there was no correlation between expression of eGFP and that of the functional markers NKp46, Granzyme B, or Ly49c (Fig. 1G). The flow cytometry gating strategy used to generate the data shown in Fig. 1C–1E is depicted in Supplementary Figure S2D.

To confirm these findings, we conducted Western immunoblots to directly evaluate CaMKK2 protein expression. Splenic NK cells were cultured in EO771 TCM and subsequently analyzed for CaMKK2 expression. TCM is exhausted media recovered from tumor cells grown *in vitro*, and it offers a controlled approximation of the tumor microenvironment. BMDMs were propagated from WT and CaMKK2 KO mice and used as a positive control on the Western blots. We found that CaMKK2 was robustly expressed in TCM-treated NK cells harvested from CaMKK2-eGFP reporter mice and the equivalent cells from WT BL/6 mice (Fig. 1H–I). In both models, NK cells cultured in normal media exhibited a low baseline level of CaMKK2 expression (Fig. 1H–I). The observation that CaMKK2 protein levels in CaMKK2-eGFP reporter NK cells strongly correlated with levels of eGFP fluorescence (Fig. 1H) validated the reporter mouse model. Moreover, CaMKK2 protein was undetectable in T cells under any conditions (Fig. 1I). These findings indicate that CaMKK2 expression is significantly upregulated in NK cells under tumor conditions, a phenomenon that is not generalizable among lymphocytes.

Ablation of NK cell–intrinsic CaMKK2 enhances metastatic tumor growth in multiple tumor models

Given the clinical importance of metastatic disease and the central role of NK cells in regulating metastatic progression [31], we assessed the relevance of NK cell–intrinsic CaMKK2 expression in animal models of metastasis. To limit CaMKK2 ablation to the NK-cell compartment, our initial experiments utilized NSG mice reconstituted with splenic NK cells from WT or CaMKK2 KO mice (Fig. 2A). CaMKK2 ablation did not affect NK-cell development, as the prevalence, absolute number, and maturation state of NK cells were comparable in WT and CaMKK2 KO animals (Supplementary Fig. S3). Moreover, the WT and CaMKK2 KO NK cells were qualitatively similar at the time of transfusion, as assessed by the expression of activation and maturation markers (Supplementary Fig. S3). To increase tumor cell sensitivity to NK-cell killing, the EO771 tumor line was engineered to eliminate the expression of major histocompatibility complex class I (MHC I) using a CRISPR-based approach to delete both alleles of β2m (Supplementary Fig. S3A). The EO771 cells were also modified to express luciferase, enabling systemic monitoring of tumor burden using a luciferin-based *in vivo* imaging system (IVIS). To induce metastasis, the modified EO771 cells were injected via tail vein. Within two weeks of tumor injection, mice reconstituted with CaMKK2 KO NK cells exhibited a significantly larger systemic EO771 metastatic burden than mice reconstituted with WT NK cells (Fig. 2B), suggesting that ablation of CaMKK2 in NK cells impairs their ability to eliminate metastatic cells.

The metastasis study was repeated using B16-F10 melanoma cells, which express low levels of MHC I (Supplementary Fig. S3A). In this model, mice reconstituted with CaMKK2 KO NK cells also exhibited a significantly larger metastatic B16-F10 burden compared to their WT counterparts (Fig. 2C). Post-mortem flow cytometry analysis of the lung tissue, which was the dominant site of metastasis, showed a significant reduction in the viability and prevalence of NK cells in the lungs of the CaMKK2 KO group (Fig. 2D). However, the WT and CaMKK2 KO groups exhibited no differences in the expression of NK-cell activation and maturation markers (Fig. 2E). These results suggest that NK-cell viability, but not cytotoxic function, is compromised upon CaMKK2 ablation.

The CaMKK2 KO NK cells transfused in the metastasis studies described in Figure 2 were harvested from animals with a germline deletion of the CaMKK2 locus, raising the possibility of confounding developmental or compensatory factors. To control for these factors, we repeated the metastasis experiments using a tamoxifen-inducible CaMKK2 KO model. This model features constitutive expression of a cre-ERT2 fusion protein that translocates to the nucleus upon tamoxifen induction, excising the floxed *Camkk2* alleles (Fig. 3A). Splenic NK cells were harvested from $ERT2^+$ and $ERT2^-$ controls after one week of tamoxifen induction, and the NK cells were co-transfused with luciferase-expressing B16-F10 cells into NSG hosts. Knockdown of CaMKK2 in BMDMs from $ERT2^+$ mice, and retained expression in the $ERT2^-$ mice, was confirmed by Western immunoblot (Supplementary Fig. S3E). Within two weeks of tumor injection, mice reconstituted with the $ERT2^+$ NK cells showed a significantly larger systemic B16-F10 tumor burden compared to the $ERT2^-$ controls (Fig. 3B–C).

Post-mortem flow cytometry analysis of the immune cell repertoire in the lungs showed a reduction in total live NK cells in the $ERT2^+$ group compared to that observed in $ERT2^-$ mice (Fig. 3D), as was observed in the prior studies using the germline CaMKK2 KO model (Fig. 2D). The reduction in live NK cells is likely driven by reduced proliferation, reflected in lower Ki67 expression among $ERT2^+$ NK cells, and by a reduction in NK-cell viability in the $ERT2^+$ group (Fig. 3D). We measured MHC I expression on recovered tumor cells and found a dramatic increase in the expression of this protein in the $ERT2^-$ group compared to the $ERT2^+$ group (Fig. 3E). MHC I expression protects tumors from NK cell–mediated killing, so MHC I upregulation is likely the result of selective pressure exerted on the tumor cells by NK cells. Thus, persistently low MHC I expression on the tumors provides direct evidence of reduced immunoediting when NK cells lose CaMKK2 expression.

The metastasis studies conducted to this point utilized immune deficient NSG mice in which transfused NK cells were the only functional bone marrow–derived immune population. However, many other immune populations are normally present in the tumor microenvironment, and these populations may affect the overall phenotype or be impacted by the loss of CaMKK2 in NK cells. Thus, we developed a model in which CaMKK2 was specifically ablated in NK cells in immune competent animals (Fig. 3F). Specifically, we crossed mice with floxed CaMKK2 alleles to mice expressing *cre* under the control of the NKp46 promoter, which is only active in NK cells. Experimental and control mice both expressed one copy of the NKp46-cre construct, but only the experimental group contained floxed *Camkk2* alleles. These mice were injected via tail vein with luciferase-expressing

B16-F10 tumor cells, and within two weeks of tumor administration, the experimental group exhibited a significantly larger systemic B16-F10 tumor burden than control mice (Fig. 3G–H). These studies revealed that ablation of CaMKK2 in the NK-cell compartment reduced immune surveillance in immune competent animals. Extensive immune profiling of post-mortem lung tissue was performed, but we did not identify any other immunologic changes resulting from NK cell–specific CaMKK2 ablation (Supplementary Fig. S3F). Thus, the reduced tumor burden associated with CaMKK2 expression in NK cells is likely mediated by direct changes in the size of the NK-cell population.

CaMKK2 expression preserves viability and proliferative capacity of NK cells

To further elucidate the role of CaMKK2 in NK-cell biology, we conducted a series of *in vitro* assays using splenic NK cells cultured in TCM. Two models of CaMKK2 ablation were employed for these *in vitro* studies: first, NK cells harvested from WT and CaMKK2 KO mice; and second pharmacologic ablation of CaMKK2 in WT NK cells using the CaMKK2 LDD CC3240 (Supplementary Fig. S1). This LDD degrades about 75% of the CaMKK2 protein in primary mouse NK cells (Supplementary Fig. S4A).

Both CaMKK2 KO and CC3240-treated groups, when exposed to TCM, exhibited a significant reduction in total number of live NK cells compared to the WT and DMSO controls (Fig. 4), likely driven by a combination of increased NK-cell apoptosis and reduced proliferation. When cultured in TCM, both KO and CC3240-treated NK cells showed significantly reduced viability (Fig. 4) and increased levels of Annexin V staining compared to controls (Fig. 4). Similar results were observed when TCM from A7C11 cells was used in place of EO771 TCM (Supplementary Fig. S4B). Moreover, CaMKK2 KO NK cells cultured in TCM exhibited reduced expression of the proliferation marker Ki67 compared to WT NK cells (Fig. 4D). To directly measure proliferation, WT NK cells were stained with CFSE vital dye and cultured in TCM with CC3240 or DMSO vehicle. CFSE is diluted with each round of cell division, so reduced CFSE fluorescence serves as a proxy for proliferation. We found that the CC3240-treated NK cells were significantly less likely to undergo division compared to the DMSO-treated control cells (Fig. 4H), further indicating that CaMKK2 expression preserves proliferative capacity. In addition, exposure to TCM was required to elicit the noted differences in survival and proliferation (Fig. 4A–H, Supplementary S4).

The impact of CaMKK2 on NK-cell migration was also assessed. To this end, WT NK cells were cultured in TCM with CC3240 or DMSO vehicle for 72 hours, at which point equal numbers of live cells from each group were placed into the upper inserts of a migration chamber containing the CCL4 chemokine in the lower well. After three hours, it was observed that significantly fewer CC3240-treated NK cells had migrated to the bottom chamber compared to the DMSO control (Supplementary Fig. S4C). WT and CaMKK2 KO NK cells expressed CCR5, the CCL4 receptor, at comparable levels (Supplementary Fig. S4D). These data, together with that from the cell survival and proliferation studies, suggest that CaMKK2 expression confers a general fitness advantage on tumor-conditioned NK cells.

The effects of CaMKK2 expression on the cytotoxic actions of NK cells were also assessed. We determined that CaMKK2 ablation had no effect on the expression of several functional markers in TCM-treated NK cells, including NKG2D, Ly49c, and CD27 (Fig. 4I). These results were consistent with the activation marker profile on WT and CaMKK2 KO NK cells recovered from murine lung metastases (Fig. 2E). We also evaluated the direct cytotoxicity of CaMKK2 KO and CC3240-treated NK cells. Specifically, NK cells were cultured in TCM with CC3240 or DMSO vehicle, then co-cultured with YAC-1 target cells at fixed ratios, and the survival of YAC-1 cells was measured. Neither pharmacologic ablation of CaMKK2 (Fig. 4J) nor genetic ablation of CaMKK2 (Supplementary Fig. S4E) affected the cytotoxicity of NK cells against YAC-1 tumors. Together, these results suggest that CaMKK2 regulates apoptosis, proliferation, and movement of NK cells without directly affecting their cytotoxic potency.

To study the mechanism by which CaMKK2 regulates NK-cell functions, we compared the effects of several functionally distinct CaMKK2-modulating compounds. CC8977, YL-36, and GSKi are high-affinity CaMKK2-specific kinase inhibitors that do not affect CaMKK2 protein levels, whereas the LDDs CC3240 and CC3756 recruit the E3 ubiquitin ligase von Hippel-Lindau (VHL) to degrade CaMKK2 protein, mimicking genetic ablation of *Camkk2*. Only the LDDs reduced the viability of TCM-treated NK cells (Fig. 4K, Supplementary S4G) and expression of Ki67 (Supplementary Fig. S4H–I). These results are consistent with a potential scaffolding function for CaMKK2 in tumor-conditioned NK cells as loss of kinase activity did not replicate the effects of protein degradation. We also treated tumor-conditioned NK cells with the most widely used competitive CaMKK2 kinase inhibitor STO609, but this drug was found to reduce NK-cell survival even under normal media conditions (Supplementary Fig. S4F), likely reflecting its lack of target specificity at the concentrations needed for quantitative inhibition of CaMKK2 [21].

The mTOR and IL15 pathways are ubiquitous regulators of NK-cell survival and proliferation [32], and we hypothesized that CaMKK2 may activate one of these pathways. However, we observed no effect of LDD-mediated CaMKK2 ablation on pSTAT5 levels, which is the primary relay downstream of the IL15 receptor (Supplementary Fig. S4J). Although LDD treatment increased phosphorylation of S6 Kinase, a downstream target of the mTOR complex, this increase was also observed when NK cells were treated with competitive CaMKK2 inhibitors (Supplementary Fig. S4J). Thus, the CaMKK2 scaffold does not appear to regulate NK-cell fitness through the IL15 or mTOR pathways, but rather through an as yet unidentified pathway.

Lactic acid exposure results in increased CaMKK2 expression in NK cells

The finding that exposure to TCM resulted in a robust upregulation of CaMKK2 in NK cells, suggested that soluble factors produced by tumor cells could mediate this adaptive activity. To distinguish between protein signaling factors and small molecule factors, we repeated the *in vitro* NK-cell survival assay using heat-inactivated TCM in which protein factors are denatured. NK cells cultured with heat-inactivated TCM and treated with CC3240 exhibited the same reduction in viability as NK cells cultured with normal TCM and CC3240 (Supplementary Fig. S5A), indicating that the factors responsible for CaMKK2 upregulation

were likely a non-proteinaceous small molecule(s). Unbiased mass spectrometry-based metabolic profiling of two TCM samples (A7C11 and EO771) was used to identify small molecule factors that may increase CaMKK2 expression [33]. In this manner, we identified twelve metabolites that were most significantly upregulated in both TCM samples compared to normal growth media (Supplementary Fig. S5B).

To assay the role of lactic caid in CaMKK2 expression, splenic NK cells from CaMKK2 reporter mice were cultured in normal growth media, EO771 TCM, or 10 mM lactic acid, a concentration found in solid tumors [34]. It was determined that eGFP expression increases significantly in the lactic acid and TCM groups, but not in the normal media group (Fig. 5A). Thus, lactic acid was sufficient to induce CaMKK2 expression. Lactic acid could mediate this effect through several mechanisms, including GPCR engagement, acidification, or direct intracellular activity. We found that the canonical cell-surface lactate receptor GPR81 was not expressed on any subset of NK cells (Supplementary Fig. S5), but the lactate transport channel monocarboxylate transporter 1 (MCT1) was expressed in NK cells (Supplementary Fig. S5). Inhibition of MCT1 with the competitive antagonist AZD3965 prevented eGFP upregulation in CaMKK2 reporter NK cells cultured in lactic acid–rich media (Fig. 5B), suggesting that lactate works intracellularly to regulate CaMKK2 expression.

Using Western immunoblots, we determined that lactic acid–treated NK cells robustly expressed CaMKK2 protein compared to the modest baseline levels in cells cultured in normal media (Fig. 5C). Moreover, treating the NK cells with AZD3965 or with the pan-MCT inhibitor αCHC significantly reduced CaMKK2 expression (Fig. 5C). To control for the effects of media acidification, the NK cells used in these studies were cultured in heavily buffered media (pH of 7.4), and no upregulation of CaMKK2 was observed when NK cells were cultured in media with a fixed pH of 6.4 (Fig. 5C). These data suggest that CaMKK2 upregulation is the product of direct lactic acid signaling (or metabolism) rather than an indirect effect of media acidification. The role of lactic acid signaling in CaMKK2 modulation was further demonstrated using survival and proliferation assays comparing the effects of TCM and lactic acid on NK cells. Lactic acid reduced the viability of CC3240-treated NK cells in the same manner as TCM (Fig. 5D), while also reducing expression of the Ki67 proliferation marker in CC3240-treated NK cells (Fig. 5E). These data are consistent with the hypothesis that upregulation of CaMKK2 expression is a response to intratumoral lactic acid accumulation.

DISCUSSION:

MHC I is expressed on all nucleated cells to present intracellular antigens for immune interrogation, but many tumors downregulate expression of this ubiquitous complex to hide their mutated neo-antigens from cytotoxic T cells [35]. Such tumors become targets for NK cells, which attack MHC I^{low} cells expressing markers of DNA damage common in tumors, such as MICA, MICB, and ULBP1-3 [36]. NK cells also mediate antibody-dependent cellular cytotoxicity (ADCC), a process that destroys antibody-opsonized targets [37, 38]. However, pro-tumor NK-cell subsets have also been identified, including “decidua-like” NK

cells that produce high levels of pro-angiogenic factors [39] and “regulatory” NK cells that suppress immune activity through cytokine production [40].

Given their multifaceted role in tumor immunity, there has been considerable interest in manipulating NK cells for therapeutic benefit, but there are significant challenges to this approach. Transfusions of autologous cytokine-primed NK cells or highly active human NK-cell lines, such as the lymphoma line NK92, have been attempted with some success [41, 42]. However, immune suppression within the tumor microenvironment is a limiting factor [43]. Solid tumors are often hypoxic, nutrient-depleted, and replete with immunosuppressive factors such as TGFβ and activin, which disable NK-cell activation and proliferation [44, 45]. Long considered a waste product of anerobic metabolism, lactic acid is now appreciated as an important immunosuppressive signaling molecule in the tumor microenvironment. Lactic acid promotes M2 macrophage polarization through HIF1α signaling [46], reduces MHC class II expression on dendritic cells [47], and suppresses the activation and survival of T cells and NK cells [48].

In this study, we have determined that lactic acid facilitates the upregulation of CaMKK2 expression in NK cells, enhancing survival while facilitating proliferation, and thereby mitigating the suppressive effects of the lactic acid-rich tumor microenvironment. Our data specifically support a role for intracellular lactate in the regulation of CaMKK2 as the actions of lactic acid (a) are blocked by inhibitors of the MCT lactate transporters, (b) are not mimicked by general acidification, and (c) do not appear to require cell surface lactate receptors. We have not yet identified the specific mechanism(s) by which intracellular lactate modulates CaMKK2 expression, although work from other groups is instructive in this regard. Lactic acid may exert direct effects on transcription by (a) functioning as a competitive inhibitor for several histone deacetylases (HDACs) [49], (b) regulating the activity of HIF-1α [50], or (c) directly modifying histone function through lactylation of lysine residues [51]. Our data do not exclude a contributory role for other tumor metabolites or for cell–cell interactions, but rather establish a prominent role for lactic acid.

Although a large body of evidence indicates that NK cells play a pivotal role in the antitumor immune response, the function of NK cells in the primary tumor varies with tumor type [52, 53]. More consistent evidence indicates a key role for NK cells in metastatic disease [31]. For this reason, we investigated the function of NK-cell intrinsic CaMKK2 in the context of tumor metastasis. Studies performed using two different tumor lines and three models of CaMKK2 ablation demonstrated that deletion of CaMKK2 in NK cells results in decreased survival and proliferation of NK cells, enabling metastatic progression. We have not probed the role of CaMKK2 in the function of human NK cells, but single cell mRNA sequencing of human tumors may be informative in this regard.

The contrasting effects of CaMKK2 inhibitors and LDDs on NK-cell survival support a distinct “scaffolding” function independent of CaMKK2’s enzymatic activity. Several proteins are known to bind CaMKK2, including the eponymous calmodulin activator and the inhibitory 14-3-3γ protein [3, 54]. CaMKK2 serves an important scaffolding function in hepatocellular carcinoma, nucleating the assembly of a CaMKIV, mTOR, and S6K complex that promotes tumor proliferation [55]. However, this specific scaffold complex is unlikely

to account for CaMKK2 activity in NK cells as it also requires the kinase function of the enzyme. We established that neither the mTOR pathway nor the IL15 pathway is affected by CaMKK2 ablation in NK cells.

Our work has therapeutic implications as it reveals potential liabilities associated with the inhibition of MCT1 and CaMKK2, while suggesting novel strategies for enhancing NK-cell immunity. By blocking the accumulation of intracellular lactate in NK cells, MCT1 inhibitors may reduce CaMKK2 upregulation, limiting the utility of this class of drugs in NK cell–sensitive tumors. In a similar manner, the detrimental effects of LDD-mediated CaMKK2 ablation in NK cells may attenuate the established benefits of CaMKK2 ablation in tumor cells and TAMs [17]. However, we did not observe any negative effects of competitive CaMKK2 inhibitors on NK cells, indicating that loss of the CaMKK2 scaffold function, but not inhibition of kinase function, is deleterious to NK-cell immunity. Thus, competitive inhibitors of CaMKK2 may be clinically preferable to LDDs. NK-cell transfusions are being investigated as a cancer therapy, and our findings suggest that modification of these immune cells to constitutively express CaMKK2 may confer proactive resistance to the suppressive effects of the tumor microenvironment. NK92 cells already robustly express CaMKK2, but primary human NK cells are also used for transfusions. Primary NK cells have been modified via retroviral transduction to overexpress receptors beneficial to antitumor activity [56, 57], and CaMKK2 could be artificially overexpressed using the same techniques.

Conclusion

We have shown that CaMKK2 is conditionally upregulated in tumor-conditioned NK cells due to lactic acid signaling, preserving NK-cell viability and proliferation in the suppressive tumor microenvironment. Indeed, CaMKK2 expression enhances NK cell–mediated immune surveillance, slowing metastatic progression in animal models. Our work suggests that CaMKK2 mediates these effects in NK cells through a scaffold function, providing the first evidence that CaMKK2 inhibitors and LDDs may confer different benefits in cancer treatment. Overall, our work elucidates an adaptive mechanism by which NK cells respond to the metabolic challenges of a lactic acid-rich environment and provide actionable insights of therapeutic relevance.

Supplementary Material

Refer to Web version on PubMed Central for supplementary material.

ACKNOWLEDGEMENTS:

This work was supported by NIH grant 1F30CA261005, NCI grant K99/R00 CA237618, Department of Defense grant W81XWH-20-1-0497, and the Duke Medical Scientist Training Program. We thank the Duke Cancer Institute Flow Cytometry Core, the Duke Optical Molecular Imaging and Analysis Service Center, the Duke Cancer Center Isolation Facility, and the Duke Molecular Physiology Institute for use of their facilities and equipment. We thank Bristol-Myers Squibb for providing compounds CC3240, CC3756, and CC8977 and Dr. David Drewry at the University of North Carolina for providing YL-36. We also thank Joseph Sun of Memorial Sloan Kettering Cancer Center for providing NKp46-iCre mice for breeding.

Financial support:

PKJ, LR, DM, SA, CYC, and DPM were funded by Department of Defense grant W81XWH-20-1-0497. PKJ was also funded by NIH grant 1F30CA261005 and the Duke Medical Scientist Training Program. XG was funded by NCI grant K99/R00 CA237618.

Conflict of interest:

DPM is a consultant for and receives research funding from BMS for projects unrelated to this work. LAD is an employee of BMS. The remaining authors have no conflicts to declare.

REFERENCES:

1. Wang J and Matosevic S, Functional and metabolic targeting of natural killer cells to solid tumors. Cell Oncol (Dordr), 2020. 43(4): p. 577–600. [PubMed: 32488848]
2. Mortezaee K, Redox tolerance and metabolic reprogramming in solid tumors. Cell Biol Int, 2021. 45(2): p. 273–286. [PubMed: 33236822]
3. Marcelo KL, Means AR, and York B, The Ca(2+)/Calmodulin/CaMKK2 Axis: Nature's Metabolic CaMshaft. Trends Endocrinol Metab, 2016. 27(10): p. 706–718. [PubMed: 27449752]
4. Racioppi L and Means AR, Calcium/calmodulin-dependent protein kinase kinase 2: roles in signaling and pathophysiology. J Biol Chem, 2012. 287(38): p. 31658–65. [PubMed: 22778263]
5. McCullough LD, et al. , Inhibition of calcium/calmodulin-dependent protein kinase kinase beta and calcium/calmodulin-dependent protein kinase IV is detrimental in cerebral ischemia. Stroke, 2013. 44(9): p. 2559–66. [PubMed: 23868268]
6. Anderson KA, et al. , Hypothalamic CaMKK2 contributes to the regulation of energy balance. Cell Metab, 2008. 7(5): p. 377–88. [PubMed: 18460329]
7. Anderson KA, et al. , Deletion of CaMKK2 from the liver lowers blood glucose and improves whole-body glucose tolerance in the mouse. Mol Endocrinol, 2012. 26(2): p. 281–91. [PubMed: 22240810]
8. Marcelo KL, et al. , Research Resource: Roles for Calcium/Calmodulin-Dependent Protein Kinase Kinase 2 (CaMKK2) in Systems Metabolism. Mol Endocrinol, 2016. 30(5): p. 557–72. [PubMed: 27003444]
9. Cary RL, et al. , Inhibition of Ca(2)(+)/calmodulin-dependent protein kinase kinase 2 stimulates osteoblast formation and inhibits osteoclast differentiation. J Bone Miner Res, 2013. 28(7): p. 1599–610. [PubMed: 23408651]
10. Jin L, et al. , The PLAG1-GDH1 Axis Promotes Anoikis Resistance and Tumor Metastasis through CamKK2-AMPK Signaling in LKB1-Deficient Lung Cancer. Mol Cell, 2018. 69(1): p. 87–99 e7. [PubMed: 29249655]
11. Frigo DE, et al. , CaM kinase kinase beta-mediated activation of the growth regulatory kinase AMPK is required for androgen-dependent migration of prostate cancer cells. Cancer Res, 2011. 71(2): p. 528–37. [PubMed: 21098087]
12. Stewart LM, et al. , CaMKK2 facilitates Golgi-associated vesicle trafficking to sustain cancer cell proliferation. Cell Death Dis, 2021. 12(11): p. 1040. [PubMed: 34725334]
13. Racioppi L, et al. , Calcium/calmodulin-dependent kinase kinase 2 regulates hematopoietic stem and progenitor cell regeneration. Cell Death Dis, 2017. 8(10): p. e3076. [PubMed: 28981105]
14. Broxmeyer HE, et al. , CaMKK2 Knockout Bone Marrow Cells Collected/Processed in Low Oxygen (Physioxia) Suggests CaMKK2 as a Hematopoietic Stem to Progenitor Differentiation Fate Determinant. Stem Cell Rev Rep, 2022.
15. Teng EC, Racioppi L, and Means AR, A cell-intrinsic role for CaMKK2 in granulocyte lineage commitment and differentiation. J Leukoc Biol, 2011. 90(5): p. 897–909. [PubMed: 21816924]
16. Racioppi L, et al. , Calcium/calmodulin-dependent protein kinase kinase 2 regulates macrophage-mediated inflammatory responses. J Biol Chem, 2012. 287(14): p. 11579–91. [PubMed: 22334678]
17. Racioppi L, et al. , CaMKK2 in myeloid cells is a key regulator of the immune-suppressive microenvironment in breast cancer. Nat Commun, 2019. 10(1): p. 2450. [PubMed: 31164648]

18. Huang W, et al. , Calcium/Calmodulin Dependent Protein Kinase Kinase 2 Regulates the Expansion of Tumor-Induced Myeloid-Derived Suppressor Cells. Front Immunol, 2021. 12: p. 754083. [PubMed: 34712241]
19. Racioppi L, CaMKK2: a novel target for shaping the androgen-regulated tumor ecosystem. Trends Mol Med, 2013. 19(2): p. 83–8. [PubMed: 23332598]
20. York B, et al. , Pharmacological inhibition of CaMKK2 with the selective antagonist STO-609 regresses NAFLD. Sci Rep, 2017. 7(1): p. 11793. [PubMed: 28924233]
21. Hawley SA, et al. , Calmodulin-dependent protein kinase kinase-beta is an alternative upstream kinase for AMP-activated protein kinase. Cell Metab, 2005. 2(1): p. 9–19. [PubMed: 16054095]
22. Burslem GM, et al. , Targeting BCR-ABL1 in Chronic Myeloid Leukemia by PROTAC-Mediated Targeted Protein Degradation. Cancer Res, 2019. 79(18): p. 4744–4753. [PubMed: 31311809]
23. Tovell H, et al. , Design and Characterization of SGK3-PROTAC1, an Isoform Specific SGK3 Kinase PROTAC Degrader. ACS Chem Biol, 2019. 14(9): p. 2024–2034. [PubMed: 31461270]
24. Tario JD Jr., et al. , Tracking immune cell proliferation and cytotoxic potential using flow cytometry. Methods Mol Biol, 2011. 699: p. 119–64. [PubMed: 21116982]
25. Gong S, et al. , A gene expression atlas of the central nervous system based on bacterial artificial chromosomes. Nature, 2003. 425(6961): p. 917–25. [PubMed: 14586460]
26. Narni-Mancinelli E, et al. , Fate mapping analysis of lymphoid cells expressing the NKp46 cell surface receptor. Proc Natl Acad Sci U S A, 2011. 108(45): p. 18324–9. [PubMed: 22021440]
27. Granzin M, et al. , Highly efficient IL-21 and feeder cell-driven ex vivo expansion of human NK cells with therapeutic activity in a xenograft mouse model of melanoma. Oncoimmunology, 2016. 5(9): p. e1219007. [PubMed: 27757317]
28. Lee J, et al. , An Antibody Designed to Improve Adoptive NK-Cell Therapy Inhibits Pancreatic Cancer Progression in a Murine Model. Cancer Immunol Res, 2019. 7(2): p. 219–229. [PubMed: 30514792]
29. Yu YR, et al. , A Protocol for the Comprehensive Flow Cytometric Analysis of Immune Cells in Normal and Inflamed Murine Non-Lymphoid Tissues. PLoS One, 2016. 11(3): p. e0150606. [PubMed: 26938654]
30. Fu B, et al. , CD11b and CD27 reflect distinct population and functional specialization in human natural killer cells. Immunology, 2011. 133(3): p. 350–9. [PubMed: 21506999]
31. Lopez-Soto A, et al. , Control of Metastasis by NK Cells. Cancer Cell, 2017. 32(2): p. 135–154. [PubMed: 28810142]
32. Nandagopal N, et al. , The Critical Role of IL-15-PI3K-mTOR Pathway in Natural Killer Cell Effector Functions. Front Immunol, 2014. 5: p. 187. [PubMed: 24795729]
33. Gao X, et al. , Serine Availability Influences Mitochondrial Dynamics and Function through Lipid Metabolism. Cell Rep, 2018. 22(13): p. 3507–3520. [PubMed: 29590619]
34. Wang JX, et al. , Lactic Acid and an Acidic Tumor Microenvironment suppress Anticancer Immunity. Int J Mol Sci, 2020. 21(21).
35. Topfer K, et al. , Tumor evasion from T cell surveillance. J Biomed Biotechnol, 2011. 2011: p. 918471. [PubMed: 22190859]
36. Sanchez-Correa B, et al. , Human NK cells in acute myeloid leukaemia patients: analysis of NK cell-activating receptors and their ligands. Cancer Immunol Immunother, 2011. 60(8): p. 1195–205. [PubMed: 21644031]
37. Wu L, et al. , lenalidomide enhances natural killer cell and monocyte-mediated antibody-dependent cellular cytotoxicity of rituximab-treated CD20+ tumor cells. Clin Cancer Res, 2008. 14(14): p. 4650–7. [PubMed: 18628480]
38. Roda JM, et al. , The activation of natural killer cell effector functions by cetuximab-coated, epidermal growth factor receptor positive tumor cells is enhanced by cytokines. Clin Cancer Res, 2007. 13(21): p. 6419–28. [PubMed: 17962339]
39. Bruno A, et al. , Angiogenin and the MMP9-TIMP2 axis are up-regulated in proangiogenic, decidual NK-like cells from patients with colorectal cancer. FASEB J, 2018. 32(10): p. 5365–5377. [PubMed: 29763380]

40. Neo SY, et al. , CD73 immune checkpoint defines regulatory NK cells within the tumor microenvironment. J Clin Invest, 2020. 130(3): p. 1185–1198. [PubMed: 31770109]
41. Parkhurst MR, et al. , Adoptive transfer of autologous natural killer cells leads to high levels of circulating natural killer cells but does not mediate tumor regression. Clin Cancer Res, 2011. 17(19): p. 6287–97. [PubMed: 21844012]
42. Tonn T, et al. , Treatment of patients with advanced cancer with the natural killer cell line NK92. Cytotherapy, 2013. 15(12): p. 1563–70. [PubMed: 24094496]
43. Veluchamy JP, et al. , The Rise of Allogeneic Natural Killer Cells As a Platform for Cancer Immunotherapy: Recent Innovations and Future Developments. Front Immunol, 2017. 8: p. 631. [PubMed: 28620386]
44. Viel S, et al. , TGF-beta inhibits the activation and functions of NK cells by repressing the mTOR pathway. Sci Signal, 2016. 9(415): p. ra19. [PubMed: 26884601]
45. Rautela J, et al. , Therapeutic blockade of activin-A improves NK cell function and antitumor immunity. Sci Signal, 2019. 12(596).
46. Colegio OR, et al. , Functional polarization of tumour-associated macrophages by tumour-derived lactic acid. Nature, 2014. 513(7519): p. 559–63. [PubMed: 25043024]
47. Brown TP, et al. , The lactate receptor GPR81 promotes breast cancer growth via a paracrine mechanism involving antigen-presenting cells in the tumor microenvironment. Oncogene, 2020. 39(16): p. 3292–3304. [PubMed: 32071396]
48. Brand A, et al. , LDHA-Associated Lactic Acid Production Blunts Tumor Immunosurveillance by T and NK Cells. Cell Metab, 2016. 24(5): p. 657–671. [PubMed: 27641098]
49. Latham T, et al. , Lactate, a product of glycolytic metabolism, inhibits histone deacetylase activity and promotes changes in gene expression. Nucleic Acids Res, 2012. 40(11): p. 4794–803. [PubMed: 22323521]
50. Kozlov AM, et al. , Lactate preconditioning promotes a HIF-1alpha-mediated metabolic shift from OXPHOS to glycolysis in normal human diploid fibroblasts. Sci Rep, 2020. 10(1): p. 8388. [PubMed: 32433492]
51. Zhang D, et al. , Metabolic regulation of gene expression by histone lactylation. Nature, 2019. 574(7779): p. 575–580. [PubMed: 31645732]
52. Habif G, et al. , Targeting natural killer cells in solid tumors. Cell Mol Immunol, 2019. 16(5): p. 415–422. [PubMed: 30911118]
53. Melaiu O, et al. , Influence of the Tumor Microenvironment on NK Cell Function in Solid Tumors. Front Immunol, 2019. 10: p. 3038. [PubMed: 32038612]
54. Lentini Santo D, et al. , Stabilization of Protein-Protein Interactions between CaMKK2 and 14-3-3 by Fusicoccins. ACS Chem Biol, 2020. 15(11): p. 3060–3071. [PubMed: 33146997]
55. Lin F, et al. , The camKK2/camKIV relay is an essential regulator of hepatic cancer. Hepatology, 2015. 62(2): p. 505–20. [PubMed: 25847065]
56. Streltsova MA, et al. , Current Approaches to Engineering of NK Cells for Cancer Immunotherapy. Curr Pharm Des, 2018. 24(24): p. 2810–2824. [PubMed: 30156154]
57. Chang YH, et al. , A chimeric receptor with NKG2D specificity enhances natural killer cell activation and killing of tumor cells. Cancer Res, 2013. 73(6): p. 1777–86. [PubMed: 23302231]

SYOPSIS:

CaMKK2 is a target being considered for anticancer therapeutic development. The authors show CaMKK2 expression preserves NK-cell fitness in the tumor microenvironment and slows the progression of metastatic tumors, findings that should be considered when applying CaMKK2-modulating therapies.

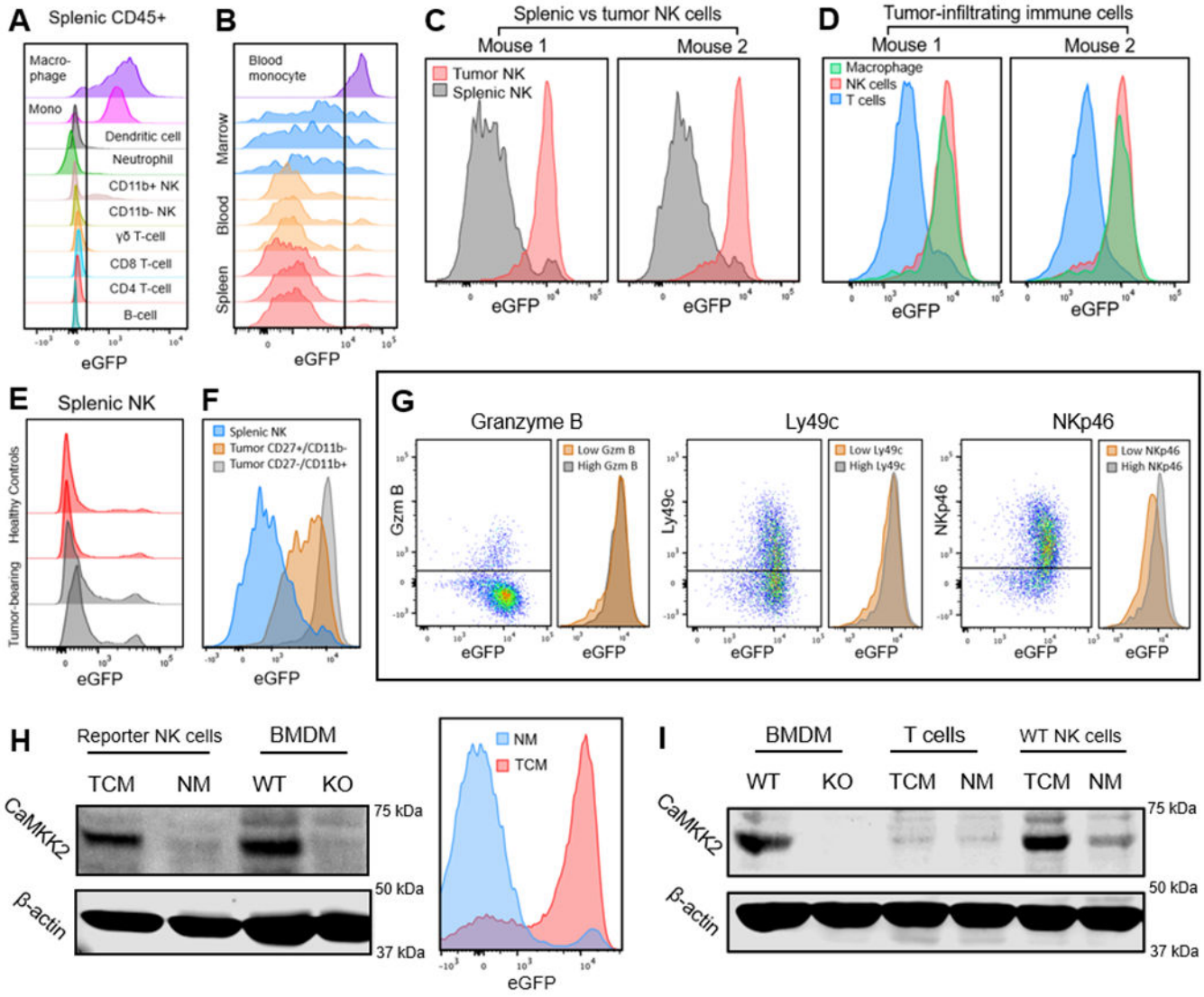

Figure 1: CaMKK2 is expressed in tumor-infiltrating NK cells.

(A) Spleens from healthy CaMKK2-eGFP reporter mice were harvested and the immune cells (defined as $CD45^+$) analyzed for eGFP fluorescence using flow cytometry according to the gating strategy in Supplementary Figure S2B. Each distribution represents >500 cells; data are representative of 2 mice in one independent experiment. (B) $CD11b^+$ NK cells were isolated from various tissues of healthy CaMKK2-eGFP reporter mice according to the gating strategy in Supplementary Figure S2C and analyzed for eGFP fluorescence using flow cytometry. Blood monocytes from the same mice are shown as a positive control. Each distribution represents >300 cells; N=3, representative of one independent experiment. (C-D) On day 14 after subcutaneous injection of EO771 cells into two CaMKK2-eGFP reporter mice, tumors and spleens were harvested and analyzed for eGFP fluorescence using flow cytometry. (C) NK cells from tumors or spleen, and (D) T cells, NK cells, and macrophages from the tumor were analyzed. Data are representative of 4 mice in two independent experiments. (E) Splenic NK cells were harvested from CaMKK2-eGFP reporter mice

bearing 14-day subcutaneous EO771 tumors and from healthy control reporter mice, and eGFP fluorescence was analyzed using flow cytometry. N=2, data representative of one experiment. (F-G) 14-day subcutaneous EO771 tumors were harvested from CaMKK2-eGFP reporter mice and eGFP expression was analyzed on a variety of tumor-infiltrating NK-cell subsets. Each distribution represents >500 cells; data are representative of 4 mice in two independent experiments. (H) Splenic NK cells were harvested from CaMKK2-eGFP reporter mice and cultured in 50% EO771 tumor-conditioned media (TCM) or normal growth media (NM) for 72 hours with IL2 and IL15 stimulation. NK cells were then analyzed for eGFP fluorescence using flow cytometry (right hand panel), and CaMKK2 and β-actin protein levels were measured by Western immunoblotting (left hand panel). BMDMs propagated from WT and CaMKK2 KO mice were used as controls to identify the CaMKK2 band. This Western represents one independent experiment. (I) Splenic T cells and splenic NK cells harvested from WT BL/6 female mice were cultured in 50% EO771 TCM or NM for 72 hours with IL2 and IL15 stimulation, and CaMKK2 and β-actin protein levels were measured by Western immunoblotting. BMDMs propagated from WT and CaMKK2 KO mice were used as controls to identify the CaMKK2 band. These data represent one independent experiment.

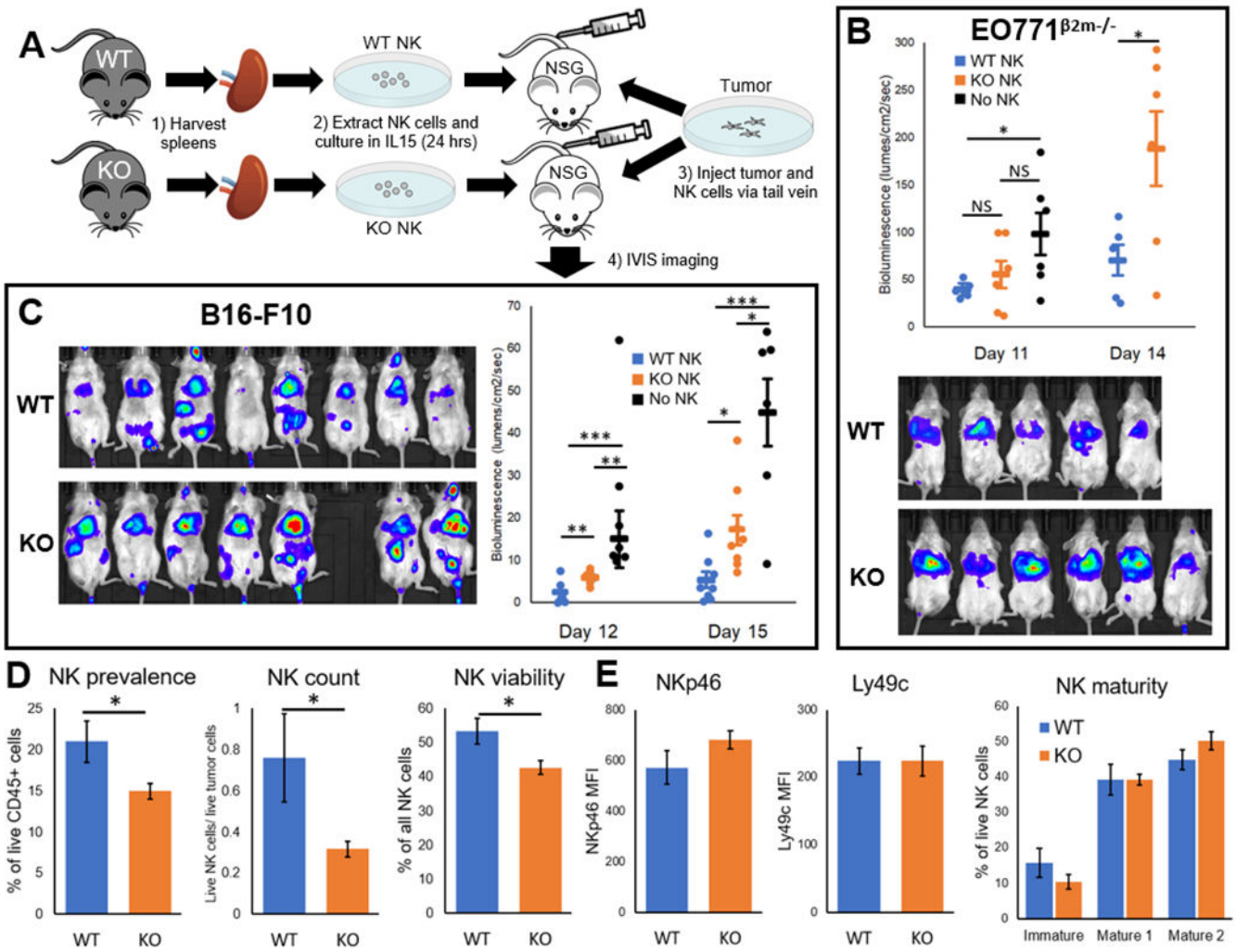

Figure 2: NK cells from CaMKK2 KO mice exhibit reduced activity against lung metastases.

(A-C) Splenic NK cells from WT or CaMKK2 KO BL/6 females were isolated, cultured in media containing IL15 for 24 hours, and intravenously transfused into NSG mice along with luciferase-expressing B16-F10 melanoma cells or luciferase-expressing $\beta2m^{-/-}$ EO771 breast tumor cells. A control group received only tumor cells and no NK cells. (B) Whole-body metastatic burden in the $\beta2m^{-/-}$ EO771 mice was measured using luciferin bioluminescence imaging. Imaging 14 days post-injection is shown in the bottom panel, and overall data from days 11 and 14 post-injection are shown in the top panel. N=5–6, standard error shown. Data are representative of one independent experiment. (C) Whole-body metastatic burden in mice receiving B16-F10 cells was measured using luciferin bioluminescence imaging. Imaging 15 days post-injection is shown in the left-hand panel, and overall data from days 12 and 15 post-injection is shown in the right-hand panel. N=7–8, standard error shown. Data are representative of two independent experiments. (D-E) NK cells were recovered post-mortem from the lungs of mice in the B16-F10 study and analyzed using flow cytometry. (D) Live NK cells as a portion of $CD45^+$ cells (NK prevalence), total live NK cells as a fraction of live tumor cells (NK count), and the fraction of all

NK cells that are alive (NK viability) were measured. (E) Median fluorescence intensity (MFI) of NKp46 and Ly49c on NK cells was measured. The distribution of immature NK cells ($CD27^{+}CD11b^{-}$), Mature 1 NK cells ($CD27^{+}CD11b^{+}$), and Mature 2 NK cells ($CD27^{-}CD11b^{+}$) was also measured. N=7–8, standard error shown. Data are representative of two independent experiments. P-values were determined using an unpaired Student's t-test with a significance threshold of $P<0.05$ (*$P<0.05$, **$P<0.01$, ***$P<0.005$).

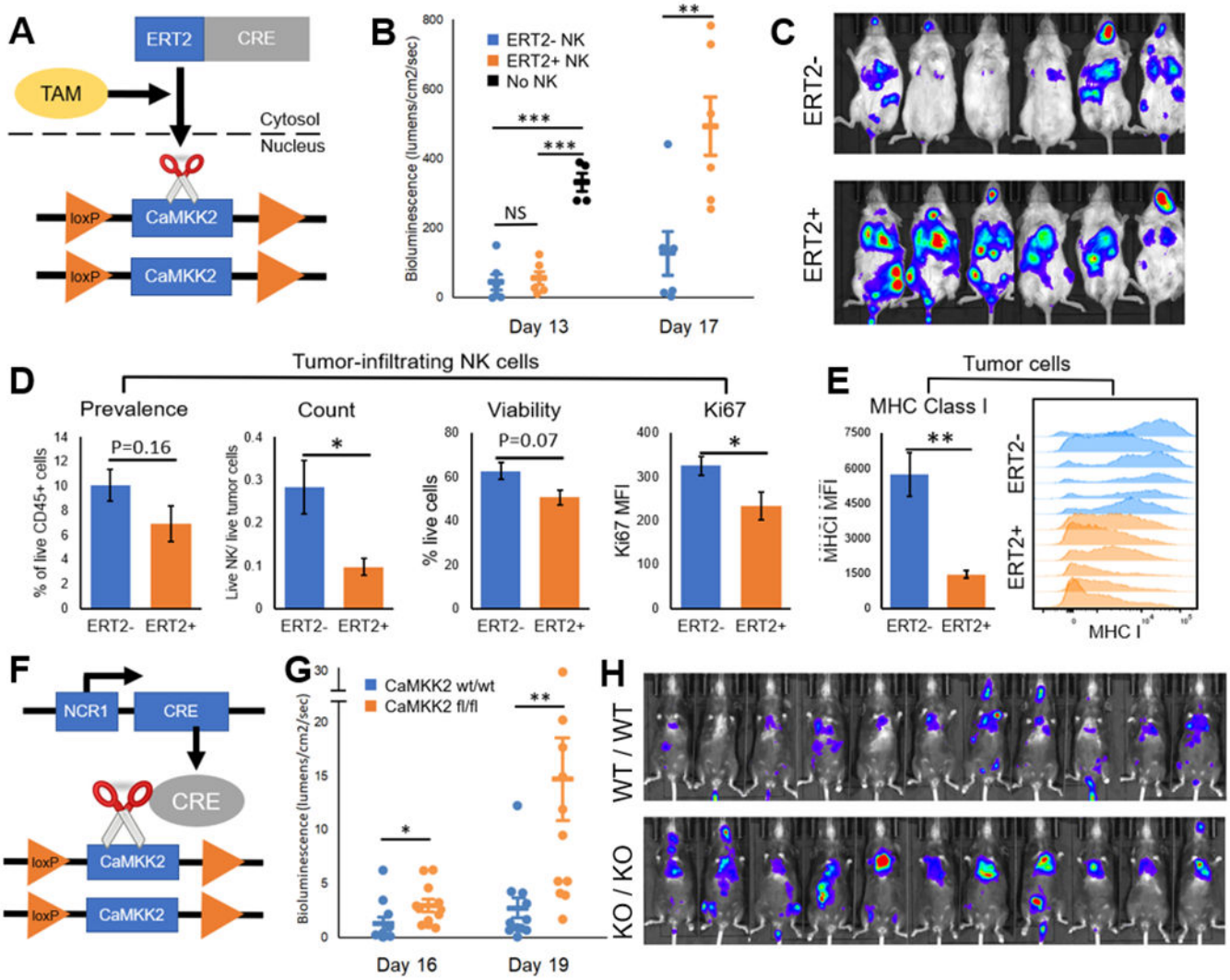

Figure 3: NK cell–intrinsic CaMKK2 ablation reduces NK-cell survival and tumor immunoediting *in vivo*.

(A-E) NK cells were harvested from the spleens of tamoxifen-treated CaMKK2$^{fl/fl}$:ERT2^{+} mice or CaMKK2$^{fl/fl}$:ERT2^{-} mice and co-injected into the tail veins of NSG mice along with luciferase-expressing GFP^{+} B16-F10 tumor cells. CaMKK2$^{fl/fl}$:ERT2^{+} mice express a fusion cre-ERT2 protein that translocates to the nucleus upon tamoxifen binding, excising the floxed CaMKK2 alleles. (B-C) Full-body luciferin bioluminescence was measured at days 13 and 17 post-injection, with imaging from day 17 shown in panel C. . N=6, standard error shown. (D) NK cells were harvested from lungs 17 days post-injection. Flow cytometry was used to measure the prevalence of NK cells among live CD45^{+} cells (prevalence), the number of live NK cells as a proportion of live tumor cells (count), the percentage of all NK cells that are alive (viability), and Ki67 expression among NK cells (Ki67). N=6, standard error shown. (E) GFP^{+} tumor cells were harvested from lungs 17 days post-injection, and MHC Class I expression was analyzed via flow cytometry. N=6, standard error shown. The flow cytometry gating strategy is depicted in Supplementary Figure S3B. Data are representative of one independent study. (F-H) Mice were bred

to express a single copy of Cre under the NKp46 promoter (iCre/+) and contain either homozygous CaMKK2$^{flox/flox}$ (FL/FL) alleles or homozygous CaMKK2$^{wt/wt}$ alleles (WT/WT). (G-H) Luciferase-expressing B16-F10 tumor cells were injected via tail vein into these two groups. Full-body luciferin bioluminescence was measured over time to track metastatic progression, with imaging from day 19 shown in panel H. N=11, standard error shown. Data are representative of two independent studies. P-value was determined using an unpaired Student's t-test with a significance threshold of $P<0.05$ (*$P<0.05$, **$P<0.01$, ***$P<0.005$).

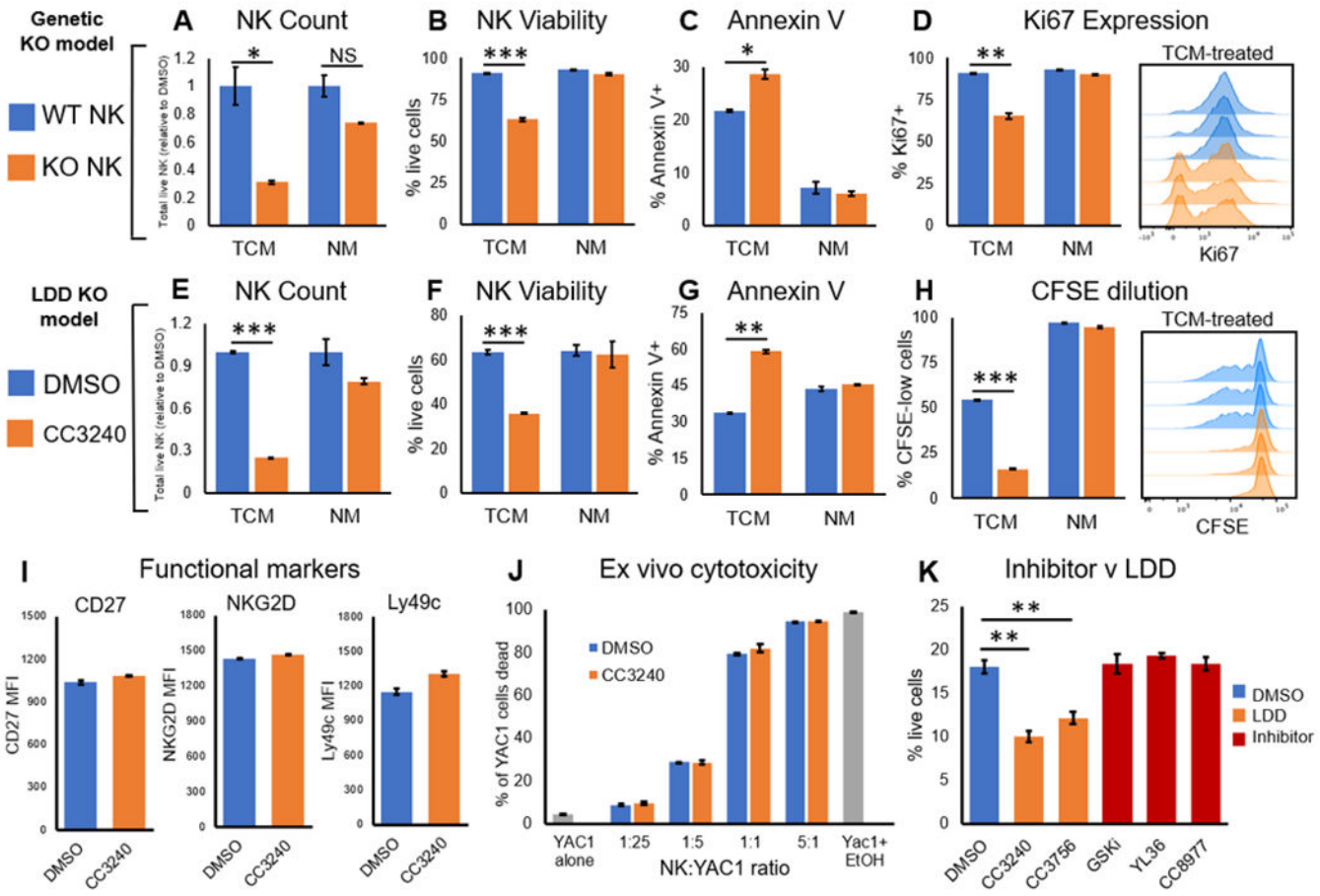

Figure 4: CaMKK2 ablation in tumor-conditioned NK cells reduces survival and proliferation.

(A-D) Splenic NK cells were isolated from WT or CaMKK2 KO BL/6 females and cultured for 96 hours in 50% EO771 TCM or normal growth media (NM) with IL2 and IL15 stimulation. Flow cytometry was used to determine (A) the total number of live NK cells as a proportion of the DMSO control, (B) the viability of the NK cells, (C) Annexin V staining on the NK cells, and (D) Ki67 expression within the NK cells. N=3, standard error shown, data are representative of two independent studies. (E-H) Splenic NK cells were isolated from WT BL/6 females and cultured for 72 hours in 50% EO771 TCM or NM containing 2.5 μM CC3240 or DMSO vehicle, with IL2 and IL15 stimulation. Flow cytometry was used to determine, (E) the total number of live NK cells as a proportion of the DMSO control, (F) the viability of the NK cells, and (G) Annexin V staining on the NK cells. (H) A portion of NK cells were stained with CFSE dye prior to *ex vivo* culture, and CFSE dilution was measured using flow cytometry at 72 hours. N=3, standard error shown, data are representative of two independent studies. (I) Splenic NK cells were isolated from WT BL/6 females and cultured for 72 hours in 50% EO771 TCM containing 2.5 μM CC3240 or DMSO vehicle, with IL2 and IL15 stimulation. The median fluorescence intensity (MFI) of key functional markers was measured using flow cytometry. N=2, standard error shown, data are representative of one independent study. (J) Splenic NK cells were isolated from WT BL/6 females and cultured for 72 hours in 50% EO771 TCM with 2.5 μM CC3240 or DMSO vehicle, with IL2 and IL15 stimulation. Live NK cells were

then co-cultured with CFSE-stained YAC-1 cells at the stated ratios for 4 hours, and YAC-1 viability was measured using flow cytometry. For controls, YAC-1 cells were cultured alone (YAC-1 alone) or with 25% ethanol (Yac1+ EtOH). N=3, standard error is shown, data are representative of one independent study. (K) Splenic NK cells were isolated from WT BL/6 females and cultured for 96 hours in 50% EO771 TCM containing DMSO vehicle, the LDD CC3240 or CC3756 (1 μM), or the competitive inhibitor GSKi, YL36, or CC8977 (1 μM). NK cells were stimulated with IL15 and IL2 throughout the assay. NK-cell viability was measured using flow cytometry. N=3, standard error shown. Data are representative of two independent studies. P-value was determined using an unpaired Student's t-test with a significance threshold of $P<0.05$ (*$P<0.05$, **$P<0.01$, ***$P<0.005$).

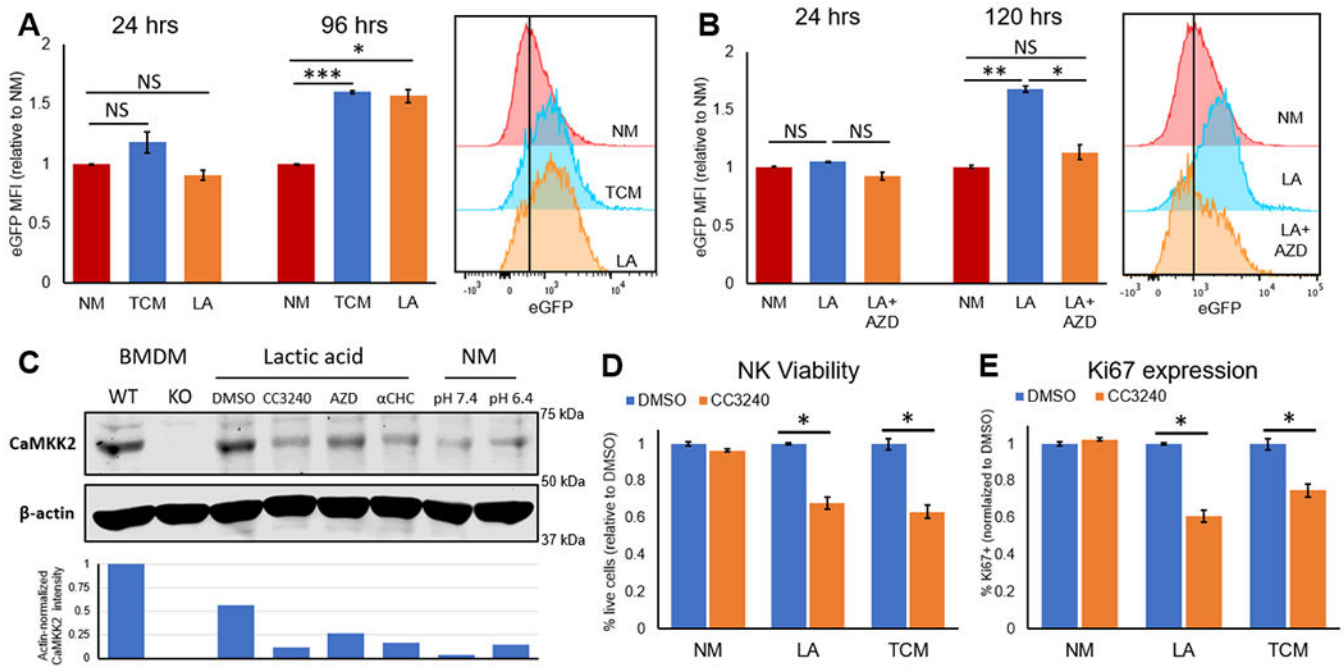

Figure 5: Lactic acid exposure causes CaMKK2 upregulation in NK cells.

(A) Splenic NK cells isolated from CaMKK2-eGFP reporter mice were cultured for 24–96 hours in normal growth media (NM), 50% EO771 tumor-conditioned media (TCM), or normal media with 10 mM lactic acid (LA). The level of eGFP expression relative to the NM group is shown at each timepoint. The eGFP fluorescence peaks at 96 hours are shown. N=3, standard error shown, data are representative of one independent study. (B) Splenic NK cells from CaMKK2-eGFP reporter mice were cultured in normal media with or without 10 mM lactic acid and with or without 500 nM AZD3965 (“AZD”) for 24–120 hours, and eGFP expression relative to the NM group is shown. The eGFP fluorescence peaks at 120 hours are shown. N=3, standard error shown, data are representative of one independent study. (C) Bone marrow-derived macrophages (BMDMs) were harvested from WT and CaMKK2 KO mice and differentiated in normal media with M-CSF. Splenic NK cells were harvested from WT BL/6 females and cultured in heavily buffered normal media with a fixed pH of 6.4 or 7.4 (“NM”) or in heavily buffered normal media with a fixed pH of 7.4 containing 10 mM lactic acid (“Lactic acid”). Various samples of lactic acid-cultured NK cells were simultaneously cultured with 2.5 μM CC3240, 500 nM AZD3965 (“AZD”), 5 mM αCHC (αCHC), or DMSO vehicle. CaMKK2 and the β-actin control were measured via Western immunoblotting (45 ug protein per lane). The Western shown is representative of two independent studies. (D-E) Splenic NK cells from WT BL/6 females were cultured in normal media (NM), 50% E0771 TCM (TCM), or normal media with 10 mM lactic acid (LA), along with 2.5 μM CC3240 or DMSO vehicle. (D) NK-cell viability and (E) expression of Ki67 are shown at 96 hours. N=3, standard error shown, data are representative of one independent study. P-value was determined using an unpaired Student’s t-test with a significance threshold of P<0.05 (*P<0.05, **P<0.01, ***P<0.005).